Histol Histopathol (2022) 37: 373-383

http://www.hh.um.es

Histology and Histopathology
From Cell Biology to Tissue Engineering

ORIGINAL ARTICLE **Open Access**

Knockdown of circular RNA hsa_circ_0062270 suppresses the progression of melanoma via downregulation of CDC45

Tian Hao[1]*, Yi Yang[2]*, Juan He[2], Jia Bai[2], Yongjian Zheng[1] and Zhanpeng Luo[3]

[1]Department of Dermatology, Beijing Younger Medical Cosmetic Hospital, [2]Department of Dermatology, The First Medical Center of Chinese PLA General Hospital and [3]Department of Orthopedic, The 8th Medical Center of Chinese PLA General Hospital, Beijing, PR China

*These authors contributed equally to this work and should be considered as co-first authors

Summary. Background. Although systemic therapies for melanoma have been improved, the 5-year survival rate of this aggressive cancer remains poor. It has been shown that hsa_circ_0062270 was upregulated in patients with melanoma. However, the relevant mechanism of hsa_circ_0062270 in the progression of melanoma remains unclear.

Methods. The CCK-8, EdU staining, flow cytometry, and transwell assays were used to determine the viability, proliferation, apoptosis and invasion in melanoma cells. An in vivo animal study was performed finally.

Results. The level of hsa_circ_0062270 was significantly upregulated in melanoma cells. In addition, hsa_circ_0062270 knockdown markedly inhibited the viability, proliferation, invasion and promoted the apoptosis of melanoma cells. Cell division cycle protein 45 (CDC45) is the host gene of hsa_circ_0062270, and downregulation of hsa_circ_0062270 notably decreased the expression of CDC45 in melanoma cells. Rescue assays confirmed that hsa_circ_0062270 regulated the growth of melanoma cells through CDC45. Moreover, immunoprecipitation (RIP) analysis showed that hsa_circ_0062270 interacted with RNA-binding protein (RBP) EIF4A3. Furthermore, in vivo study indicated that knockdown of hsa_circ_0062270 inhibited the melanoma tumor growth in vivo.

Conclusions. Downregulation of hsa_circ_0062270 can inhibit the progression of melanoma through downregulation of CDC45. Our findings provide biological mechanisms for the use of hsa_circ_0062270 as a biomarker for melanoma and potential therapeutic target.

Corresponding Author: Zhanpeng Luo, Department of Orthopedic, The 8th Medical Center of Chinese PLA General Hospital, 17 Heishan Hujia, Beijing 100094, PR China. e-mail: luozhanpeng_12@126.com

DOI: 10.14670/HH-18-412

Key words: hsa_circ_0062270, Melanoma, EIF4A3, CDC45

Introduction

Melanoma is the most aggressive form of skin cancer which manifests by uncontrolled proliferation of pigment-producing melanocytes (Chhabra et al., 2017; Matthews et al., 2017). The incidence of melanoma has climbed over the past several decades, placing this cancer on the 19th position of the most common cancer types worldwide (Matthews et al., 2017; Coricovac et al., 2018). Although early stage melanoma can be surgically removed, the treatment options for advanced melanoma are still limited (Coricovac et al., 2018). In the past decade, targeted therapies have slowly increased the survival of these patients and therefore hold great promise for the treatment of melanoma (Maverakis et al., 2015). Therefore, the development of new therapeutic targets for the treatment of melanoma is pivotal to increase the survival of patients with melanoma.

Circular RNAs (circRNAs) are a class of non-coding RNA which do not code for proteins but play critical roles in the regulation of physiological processes (Maverakis et al., 2015; Qu et al., 2017; Patop et al., 2019). CircRNA has a unique closed loop structure results from covalently joint an upstream 3'-splice site to a downstream 5'-splice site by back-splicing reaction (Starke et al., 2015; Legnini et al., 2017). In the past, circRNAs were regarded as byproducts of mRNA splicing without any functional roles (Sanger et al., 1976). However, in recent years, functional roles of circRNAs have emerged in various biological functions and pathophysiology (Fiedler et al., 2018; Zhang et al., 2020). It was found that circRNAs were associated with the occurrence and progression of numerous diseases, including cardiovascular and cerebrovascular diseases,

nervous system disorders, diabetes, and types of cancers (Rybak-Wolf et al., 2015; Salzman, 2016; Hsiao et al., 2017; Cheng and Shen, 2018; Vo et al., 2019). Thus, circRNAs are increasingly recognized as targets for developing a new generation of targeted therapeutics (Fiedler et al., 2018).

CircRNAs regulate biological processes and gene expressions at multiple levels through functional mechanisms (Zhao et al., 2019a; Nie et al., 2020). It has been shown that circRNAs interplay with RNA-binding proteins (RBPs) and can change the RNA splicing modes and mRNA stability (Nie et al., 2020). Thereby, the transcription activity of the host gene of circRNAs are regulated (Zhao et al., 2019a; Nie et al., 2020). RBPs usually contain RNA-binding motifs and play a significant role in tumorigenesis (Zhao et al., 2019b). Meanwhile, EIF4A3 was known to be a member of RBPs which has been confirmed to participate in tumor progression (Liu and Dong, 2021; Wang et al., 2021). Evidence has been found that the level of hsa_circ_0062270 was upregulated in patients with melanoma (Bian et al., 2018). However, the relation between hsa_circ_0062270 and EIF4A3 in melanoma remains to be uncovered.

Thus, this study aims to explore the function of hsa_circ_0062270 in the tumorigenesis of melanoma. The data revealed that silencing of hsa_circ_0062270 was able to inhibit the progression of melanoma through downregulation of CDC45. Therefore, hsa_circ_0062270 might serve as a novel target for treatment of melanoma.

Materials and methods

Cell culture

Melanoma cell lines A375 and MNT-1 were obtained from American Type Culture Collection (ATCC; Manassas, VA, USA). MNT-1 cells were maintained in Dulbecco's Modified Eagle's Medium (DMEM, GIBCO, NY, USA) containing 10% fetal bovine serum (FBS, GIBCO, NY, USA), 10% AIM-V (Thermo Fisher Scientific) and 0.1 mM/500 mL Nonessential Amino Acids (NEAA, 100X; Thermo Fisher Scientific). A375 cells were cultured in DMEM medium containing 10% FBS. Human epidermal melanocytes isolated from adult human skin were purchased from ScienCell (CA, USA) and cultured in Melanocyte Medium (ScienCell, CA, USA). Cell culture was carried out in a humidified incubator with 5% CO_2 at 37°C.

Cell transfection

Hsa-circ-0062270 shRNAs and negative control (NC) were constructed into pLVX by GenePharma (Shanghai, China). A375 and MNT1 cells were transfected with pLVX containing hsa-circ-0062270 shRNAs or NC for 48 h. Lipofectamine 2000 kit (Thermo Fisher) was used for transfection. The sequences of shRNAs were as follows: hsa-circ-0062270-shRNA1: 5'- GTCCTTTGTGTGTTCGGATTTCAAGAGAATCCGAACACACAAAGGACTTTTT-3'; hsa-circ-0062270-shRNA2: 5'- GCGTGCAGACTTTCAGCATTTCAAGAGAATGCTGAAAGTCTGCACGCTTTTT-3'. NC shRNA: 5'-TCTGGATGACAAGTCCAGAACCGCTTTCAAGAGAAGCGGTTCTGGACTTGTCATCCAGATTTTT-3'.

In addition, pcDNA3.1 CDC45 OE vector and control pcDNA3.1 (pcDNA3.1-ctrl) were purchased from GenePharma. A375 cells were transfected with pcDNA3.1 CDC45 OE vector or pcDNA3.1-ctrl using Lipofectamine 2000 for 48 h. After that, western blot assay was performed to verify the expression of CDC45.

RT-qPCR

Total RNA from the cultured cells were extracted using Trizol reagent (TaKaRa, Dalian, China). Then, PrimeScript RT-PCR Kit (TaKaRa) was used to synthesize cDNA from the extracted RNA. After that, qPCR was employed with SYBR Premix ExTaq™ (Takara) on an Applied Biosystems® 7500 Real-Time PCR System (Life Technologies, NY, USA). Primers were designed and synthesized by RiboBio (Guangzhou, China). The relative expression levels were calculated using the $2^{-\Delta\Delta Ct}$ method and normalized to β-actin. The thermocycler conditions were as follows: 2 mins at 95°C, 30 s at 95°C and 30 s at 65°C for 40 cycles and 30 s at 72°C. The primers used were as follows: hsa_circ_0062270, forward: 5'- TGTGTTCGGATGAAGGACATG-3', reverse: 5'- GAAGTGATCTGTCCCTGAGCC-3'; CDC45, forward: 5'- CCGCAAAGAGTTCTACGAGGT-3', reverse: 5'- CATTGACTGGCCTATGGGTGT-3'; EIF4A3, forward, 5'- GCCAGCCGAGTGCTTATTTC-3', reverse, 5'- TCTGAGGATGCGGATGTCGT-3'; β-actin, forward: 5'- GTCCACCGCAAATGCTTCTA-3', reverse, 5'-TGCTGTCACCTTCACCGTTC-3'.

Cell viability assay

Cell viability was determined using cell counting kit-8 (CCK-8, Beyotime, Shanghai, China). A375 and MNT1 cells were placed into 96-well plates at 3,000 cells/well. After that, A375 and MNT1 cells were transfected with NC or hsa_circ_0062270 shRNA1 for 48 h. Later on, 10 μl CCK-8 solution was added into each well and incubated at 37°C for 2 h. The OD value at 450 nm was detected using a plate reader.

5-ethynyl-2'-deoxyuridine (EdU) fluorescence staining

Cell-Light EdU DNA cell proliferation kit (RiboBio, Guangzhou, China) was used to measure cell proliferation following the manufacturer's instructions. Images were captured by confocal microscopy. Later on, the percentage of EdU positive cells were calculated.

Flow cytometry assay

Annexin V/propidium iodide (PI) apoptosis kit (BioVision, San Francisco, CA, USA) was used to determine cell apoptosis following the manufacture's protocol. 4×10^5 cells were harvested and resuspended in 1 ml Annexin V binding buffer. After that, cells were stained with 5 µl of Annexin V and PI in the dark at room temperature for 15 min. Subsequently, apoptotic cells were detected by flow cytometry (BD FACSAria; BD Biosciences, NJ, USA).

Transwell invasion assay

24-well transwell chambers (Corning Costar, USA) containing 8 µm pores were coated with 20 µl Matrigel (BD Bioscience, CA, USA). Cells (4×10^5/well) were resuspended in serum free medium and then placed in the upper chamber. In addition, 600 µL of DMEM with 20% FBS was used as a chemoattractant in the lower chamber. After 24 h of incubation, invading cells were fixed with 4% paraformaldehyde for 20 min and then stained with 0.1% crystal violet (Sigma-Aldrich, MO, USA). Subsequently, cells were imaged and counted under a light microscope.

Bioinformatics analysis

The analysis of CDC45 in Skin Cutaneous Melanoma (SKCM, n=461) and adjacent tissue (n=558) was performed using Gene Expression Profiling Interactive Analysis (GIEPIA) (http://gepia.cancer-pku.cn/about.html) tool based on The Cancer Genome Atlas (TCGA) database (http://tcga-data.nci.nih.gov/tcga) (Tang et al., 2017). In addition, TCGA dataset was downloaded and R analysis was performed as previously described (Colaprico et al., 2016).

Then, a TCGA dataset analyzed from GEPIA was utilized to determine whether the expression of CDC45 was associated with the overall survival of patients with melanoma as previously described (Tang et al., 2017). Meanwhile, the Kaplan-Meier curves were analyzed from GEPIA as previously described (Tang et al., 2017).

Western blot assay

A375 and MNT1 cells were lysed using RIPA buffer (Beyotime, Shanghai, China). Then, protein concentrations were quantified using the bicinchoninic acid (BCA) protein assay kit (Beyotime). Equal amounts (30 µg/lane) of protein were loaded on 10% sodium dodecylsulfate-polyacrylamide gel electrophoresis (SDS-PAGE) and then transferred onto PVDF membranes (Millipore, MA, USA). Later on, the membranes were blocked with 5% milk in TBS supplemented with 0.1% Tween-20 (TBST) for 1 h at room temperature. After that, the membranes were incubated with primary antibodies overnight at 4°C. After washing three times with PBS, the membranes were incubated with corresponding secondary antibody (1:10000, Abcam) for 1 h at room temperature. Immunoreactive blots were observed using ECL Plus reagents (GE Healthcare, Chicago, IL, USA). The antibodies used for western blots were as follows: anti-CDC45 (1:1000, Abcam), anti-cleaved caspase 3 (1:1000, Abcam), anti-EIF4A3 (1:1000, Abcam) and anti-β-actin (1:1000, Abcam).

Fluorescent in Situ Hybridization (FISH)

The localization of hsa_circ_0062270 was detected by a FISH kit obtained from RiboBio (Guangzhou, China) following the manufacture's protocol. The oligonucleotide probe for hsa_circ_0062270 was designed and provided by RiboBio as well. A375 cells were incubated with 10 µL of probe mixture overnight at 37°C. After that, cells were counterstained with DAPI. A confocal laser-scanning microscope (LSM 780, Zeiss) was used for visualization.

RNA immunoprecipitation (RIP) assay

Potential RBP of hsa_circ_0062270 was searched using Circular RNA Interactome online database (https://circinteractome.nia.nih.gov/). Then, RIP assay was carried out to verify the binding relationship between hsa_circ_0062270 and its potential RBP. Magna RIP™ RNA-Binding Protein Immunoprecipitation Kit (Merck Millipore, Billerica, MA, USA) was used for RIP assay following the manufacturer's protocol. EIF4A3 antibody (Abcam) or IgG antibody (Abcam) was used to pull down hsa_circ_0062270 in A375 cells. Finally, retrieved RNA was subjected to RT-qPCR to estimate the enrichment level of hsa_circ_0062270.

Mouse xenograft tumor model

All procedures were in accordance with the principles of the NIH Guide for Care and were approved by the Animal Care and Use Committee of the First Medical Center of Chinese PLA General Hospital (No. CA201901044). BALB/c nude mice were purchased from Vital River (Beijing, China) and divided into two groups: control group and hsa_circ_0062270 shRNA1 group. A375 cells stably expressing hsa_circ_0062270 shRNA1 cells in 100 µL PBS were injected into the flank of nude mice. The mice were sacrificed at the end of week 5. Tumor size was measured using a caliper every week, and tumor volume was calculated using the following formula: $volume=(length\times width^2)/2$. Meanwhile, tumor tissues were weighed after sacrifice.

Statistical analysis

All experiments were repeated as least in triplicate. The data are presented as means ± standard deviation (SD). Comparisons between multiple groups were subjected to analysis of One-way analysis of variance (ANOVA) followed by Tukey's test. Statistical

significance was established when P<0.05. GraphPad prism version 8.0 (Graphpad Software, La Jolla, CA, USA) was used to perform statistical analysis.

Results

Hsa_circ_0062270 knockdown suppressed the proliferation of melanoma cells

The background information of hsa_circ_0062270 is presented in Fig. 1A. It was reported that hsa_circ_0062270 was upregulated in patients with melanoma (Bian et al., 2018). In our present study, the levels of hsa_circ_0062270 in A375 and MNT1 melanoma cells were significantly upregulated compared with normal melanocytes (Fig. 1B). For the purpose of exploring the effect of hsa_circ_0062270 knockdown on the growth of melanoma cells, we used two different shRNAs (hsa_circ_0062270 shRNA1 and hsa_circ_0062270 shRNA2) to downregulate hsa_circ_0062270 in A375 and MNT1 cells. As shown in Fig. 1C,D, hsa_circ_0062270 shRNA1 achieved better knockdown efficiency compared with hsa_circ_0062270 shRNA2. Thus, hsa_circ_0062270 shRNA1 was utilized in the following experiments. In addition, the results of the CCK-8 assay indicated that the viabilities of A375 and MNT1 cells were markedly inhibited by hsa_circ_0062270 shRNA1 (Fig. 1E). Moreover, downregulation of hsa_circ_0062270 notably inhibited the proliferation of A375 and MNT1 cells (Fig. 2A,B). Taken together, hsa_circ_0062270 knockdown could suppress the proliferation of melanoma cells.

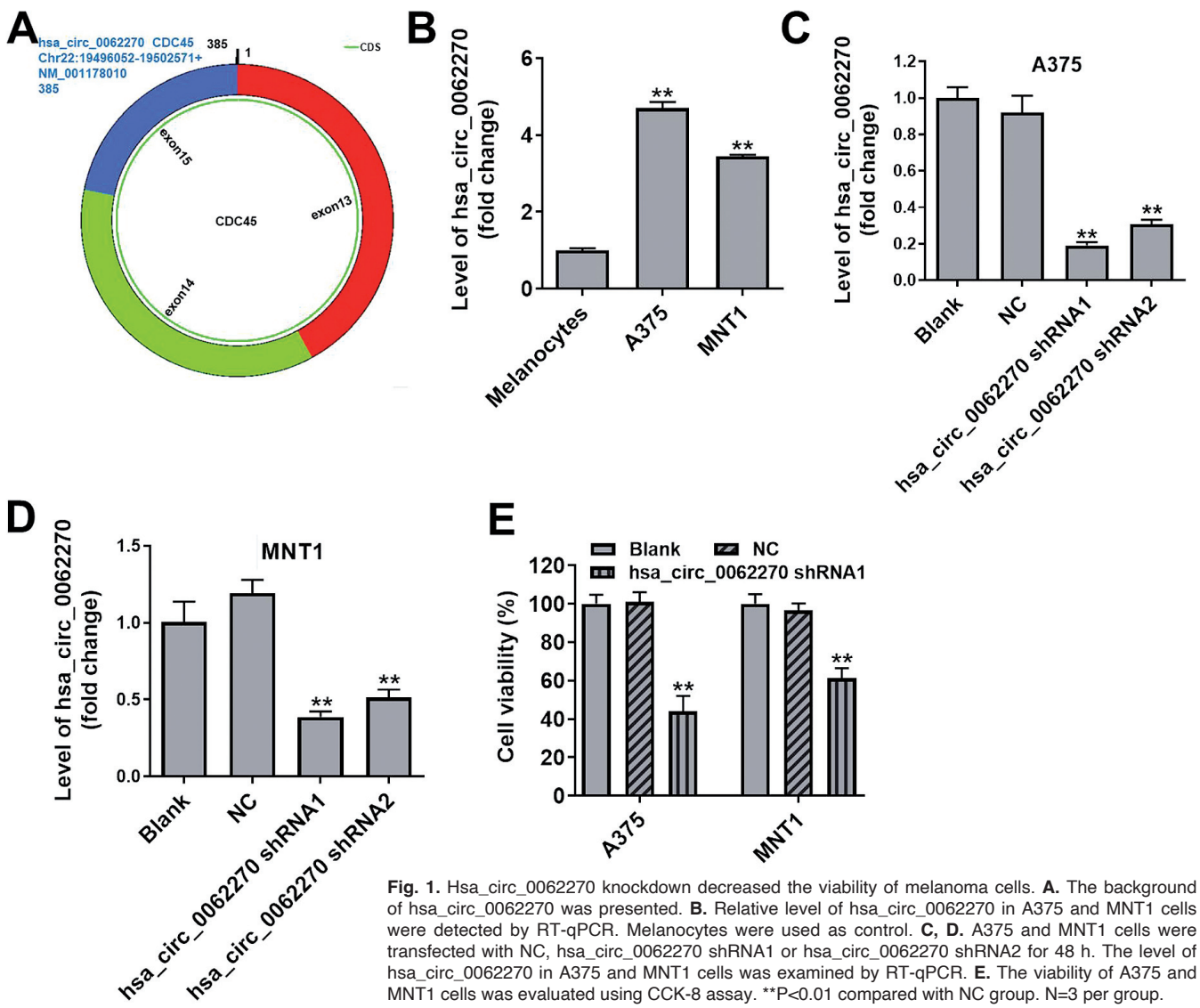

Fig. 1. Hsa_circ_0062270 knockdown decreased the viability of melanoma cells. **A.** The background of hsa_circ_0062270 was presented. **B.** Relative level of hsa_circ_0062270 in A375 and MNT1 cells were detected by RT-qPCR. Melanocytes were used as control. **C, D.** A375 and MNT1 cells were transfected with NC, hsa_circ_0062270 shRNA1 or hsa_circ_0062270 shRNA2 for 48 h. The level of hsa_circ_0062270 in A375 and MNT1 cells was examined by RT-qPCR. **E.** The viability of A375 and MNT1 cells was evaluated using CCK-8 assay. **P<0.01 compared with NC group. N=3 per group.

Hsa_circ_0062270 knockdown promoted apoptosis and reduced invasion in melanoma cells

Next, the effect of hsa_circ_0062270 shRNA1 on apoptosis and invasion was determined by flow cytometry assay and transwell assay respectively. The results of the flow cytometry assay indicated that downregulation of hsa_circ_0062270 remarkably

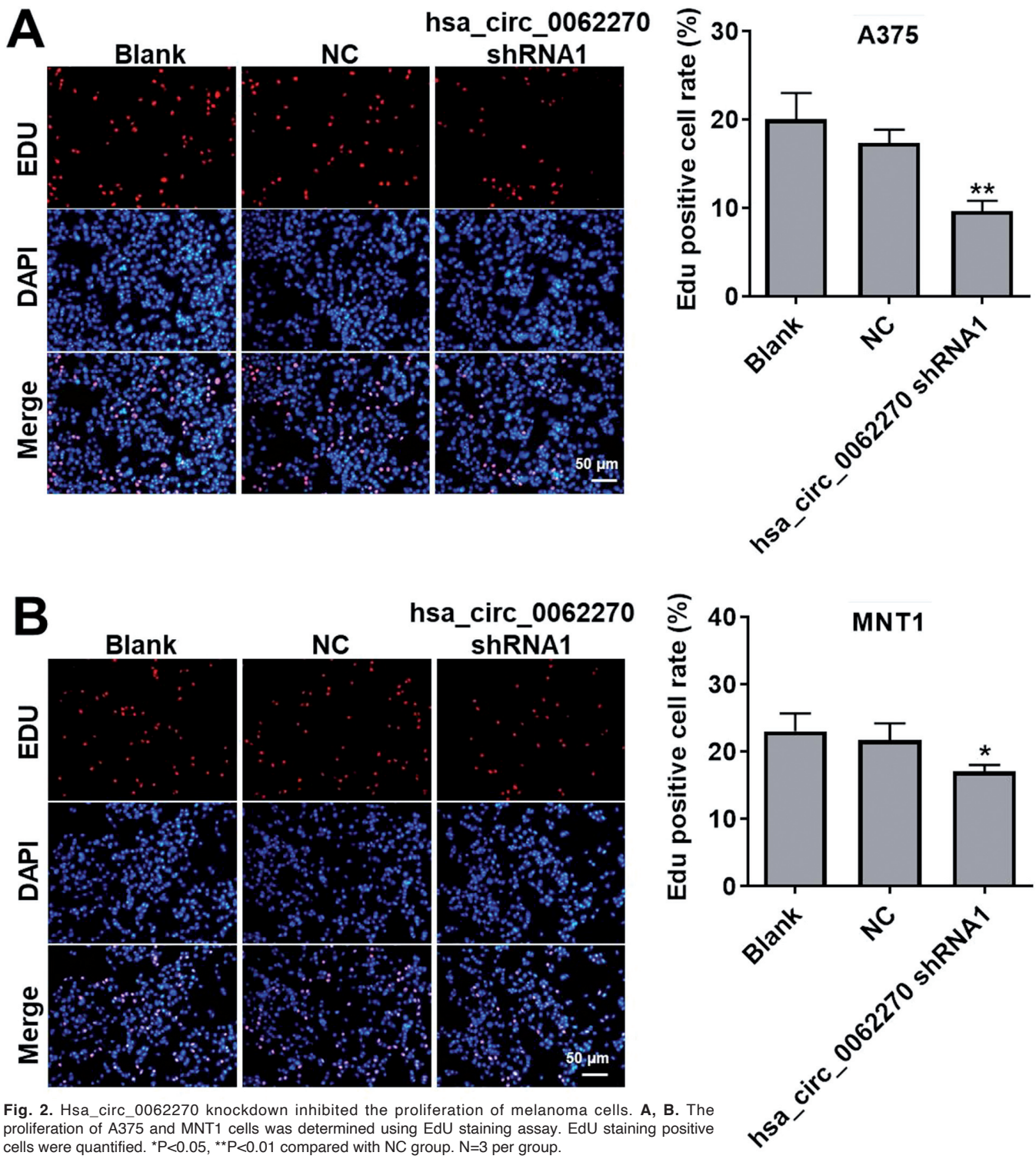

Fig. 2. Hsa_circ_0062270 knockdown inhibited the proliferation of melanoma cells. **A, B.** The proliferation of A375 and MNT1 cells was determined using EdU staining assay. EdU staining positive cells were quantified. *P<0.05, **P<0.01 compared with NC group. N=3 per group.

induced apoptosis in A375 and MNT1 cells (Fig. 3A). In addition, hsa_circ_0062270 knockdown notably suppressed the invasive ability of A375 and MNT1 cells (Fig. 3B). Taken together, Hsa_circ_0062270 knockdown was able to induce apoptosis and inhibit the invasive ability of melanoma cells.

Hsa_circ_0062270 knockdown diminished both gene and protein expression of its parental gene CDC45

CDC45 is the parental gene of hsa_circ_0062270. The level of CDC45 in melanoma and adjacent tissue was analyzed using GIEPIA (http://gepia.cancer-pku.cn/about.html) tool based on The Cancer Genome Atlas (TCGA) database (http://tcga-data.nci.nih.gov/tcga) (Tang et al., 2017). The results demonstrated that the expression of CDC45 was upregulated in melanoma tissue (Fig. 4A). Meanwhile, GIEPIA data indicated that high CDC45 level was associated with poor overall survival of patients with melanoma (Fig. 4B). In addition, RT-qPCR and western blot assays were conducted to detect the effect of hsa_circ_0062270 shRNA1 on level of CDC45 in melanoma cells. These results showed that knockdown of hsa_circ_0062270 notably decreased the mRNA and protein expression levels of CDC45 in A375 and MNT1 cells (Fig. 4C,D). These results showed that hsa_circ_0062270 knockdown was able to downregulate the expression of CDC45 in melanoma cells.

Hsa_circ_0062270 mediated melanoma cell growth through CDC45

To explore the mechanism by which hsa_circ_

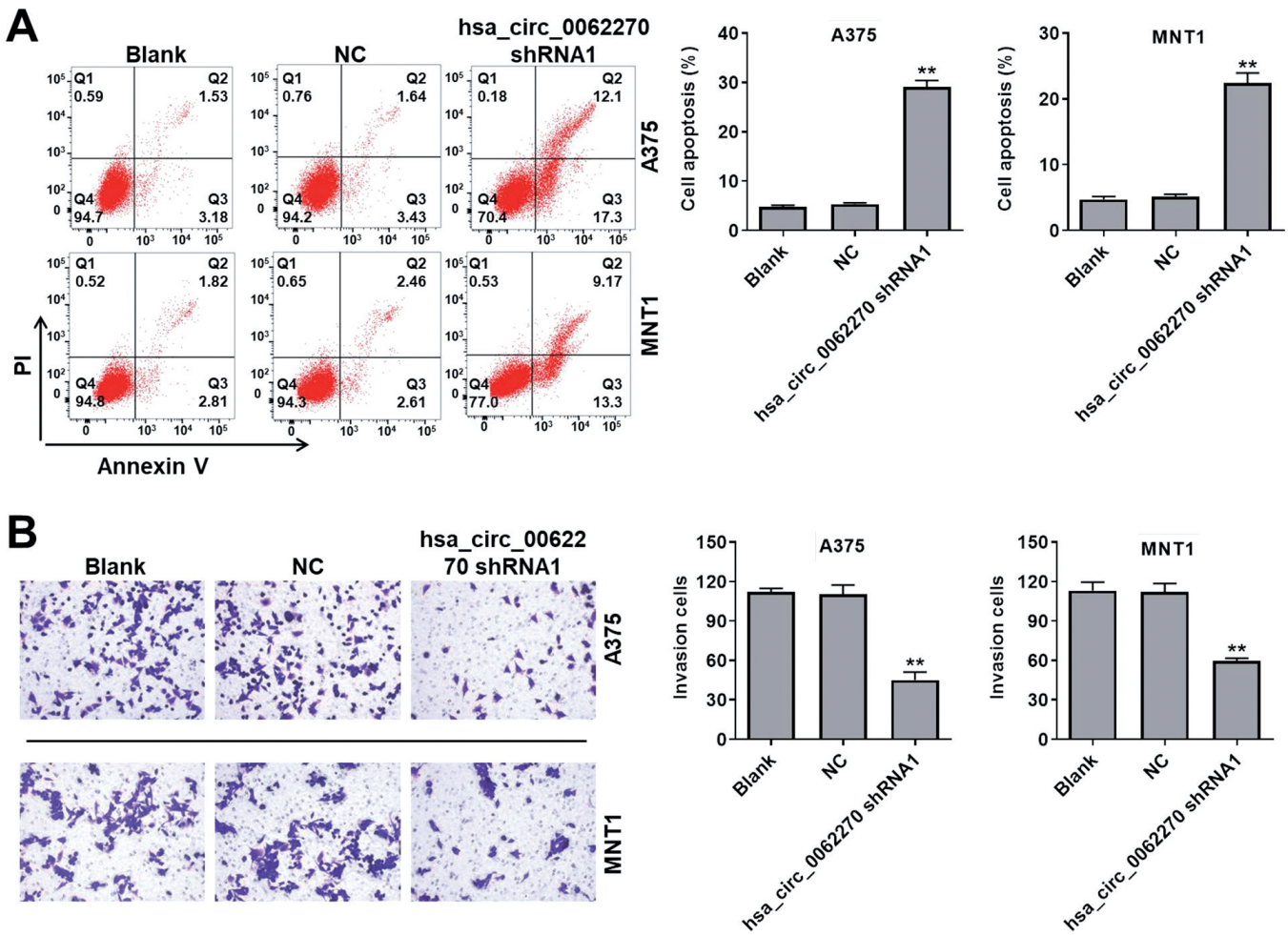

Fig. 3. Hsa_circ_0062270 knockdown promoted apoptosis and reduced invasion in melanoma cells. **A.** A375 and MNT1 cells were transfected with NC or hsa_circ_0062270 shRNA1 for 48 h. Apoptotic cells were detected with Annexin V and PI double staining. **B.** A375 and MNT1 cells were transfected with NC or hsa_circ_0062270 shRNA1 for 24 h. Transwell invasion assay was performed to determine the invasive ability of A375 and MNT1 cells. **P<0.01 compared with NC group. N=3 per group.

0062270 regulates CDC45 expression, FISH assay was performed. The results showed that hsa_circ_0062270 was partially presented in the cytoplasm (Fig. 5A). This result indicated that hsa_circ_0062270 might regulate the expression of CDC45 at post-translational level. Thus, Circular RNA Interactome database (https://circinteractome.nia.nih.gov/) was used to search potential RBPs of hsa_circ_0062270. EIF4A3 has the greatest number of matching sites to hsa_circ_0062270. Then, the potential binding relationship between EIF4A3 and hsa_circ_0062270 was verified by RIP assay followed by RT-qPCR. As shown in Fig. 5B, hsa_circ_0062270 was pulled down and enriched by anti-EIF4A3 antibody in A375 and MNT1 cells. This result verified the interaction of hsa_circ_0062270 with EIF4A3. Moreover, RT-qPCR results showed that hsa_circ_0062270 shRNA1 had no significant influence on the relative gene level of EIF4A3 in A375 and MNT1 cells (Fig. 5C).

In addition, western blot assay indicated that overexpression of CDC45 markedly upregulated the expression of CDC45 in A375 cells (Fig. 5D). Moreover, the inhibitory effect of hsa_circ_0062270 knockdown on the viability of A375 cells was reversed by CDC45 overexpression (Fig. 5E). Meanwhile, overexpression of CDC45 notably reversed hsa_circ_0062270 shRNA1-induced apoptosis of A375 cells (Fig. 5F). Furthermore, downregulation of hsa_circ_0062270 markedly decreased the expression of CDC45, and increased the expression of cleaved caspase 3 in A375 cells; however, these changes were reversed by CDC45 overexpression (Fig. 6A-C). Additionally, overexpression of CDC45 caused no change on the expression of EIF4A3 in hsa_circ_0062270 shRNA1-transfected A375 cells (Fig. 6A,D). Besides, silencing of hsa_circ_0062270 obviously decreased the mRNA stability of CDC45 (Fig.

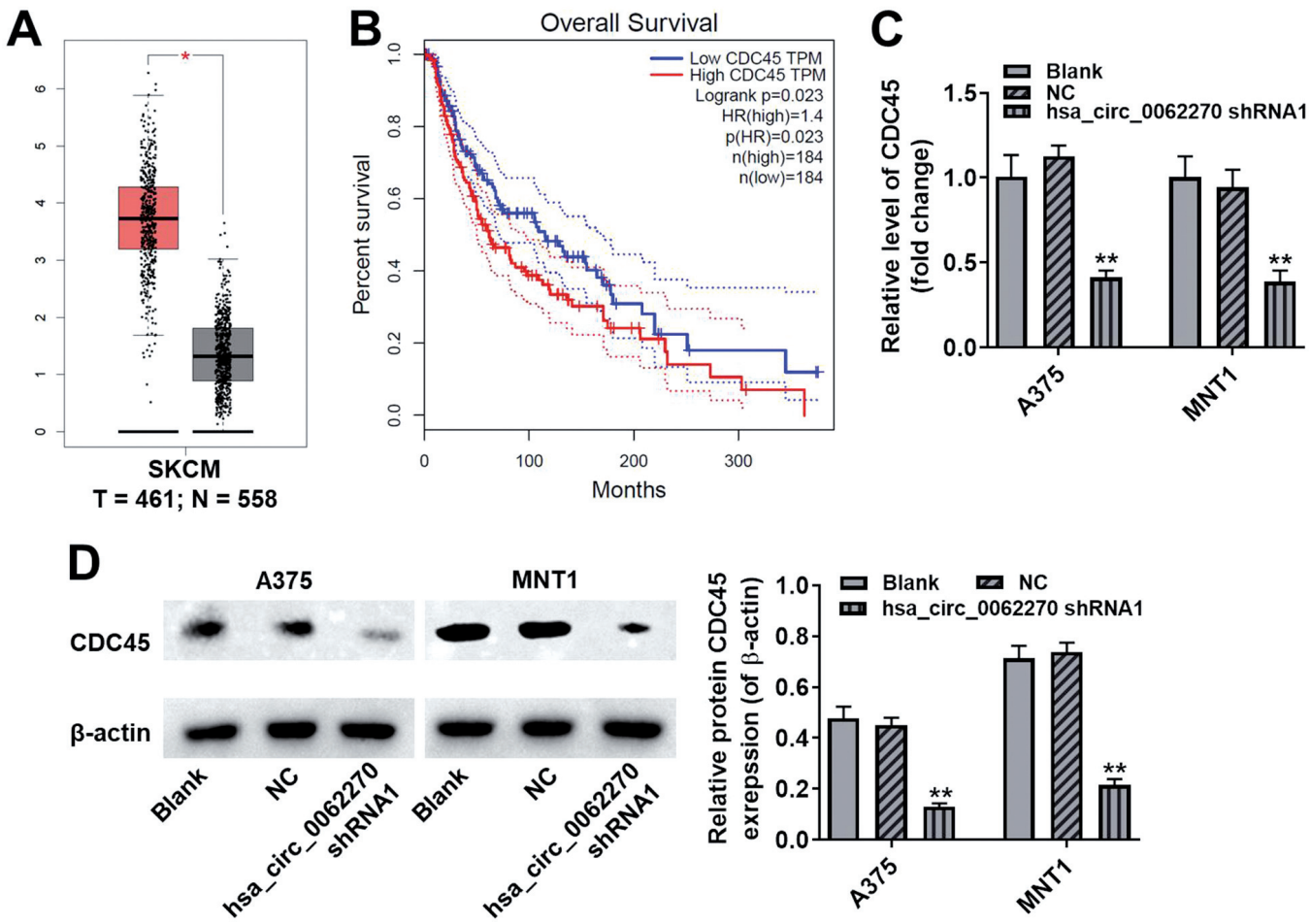

Fig. 4. Hsa_circ_0062270 knockdown diminished both gene and protein expression of CDC45. **A.** The level of hsa_circ_0062270 in melanoma (T) and adjacent tissues (N) was analyzed using GIEPIA based on TCGA database. *P<0.05. **B.** OS of patients with melanoma was analyzed using GIEPIA. **C.** A375 and MNT1 cells were transfected with NC or hsa_circ_0062270 shRNA1 for 48 h. The level of CDC45 was detected by RT-qPCR assay in A375 and MNT1 cells. **D.** The protein expression of CDC45 was determined by western blot assay. **P<0.01 compared with NC group. N=3 per group.

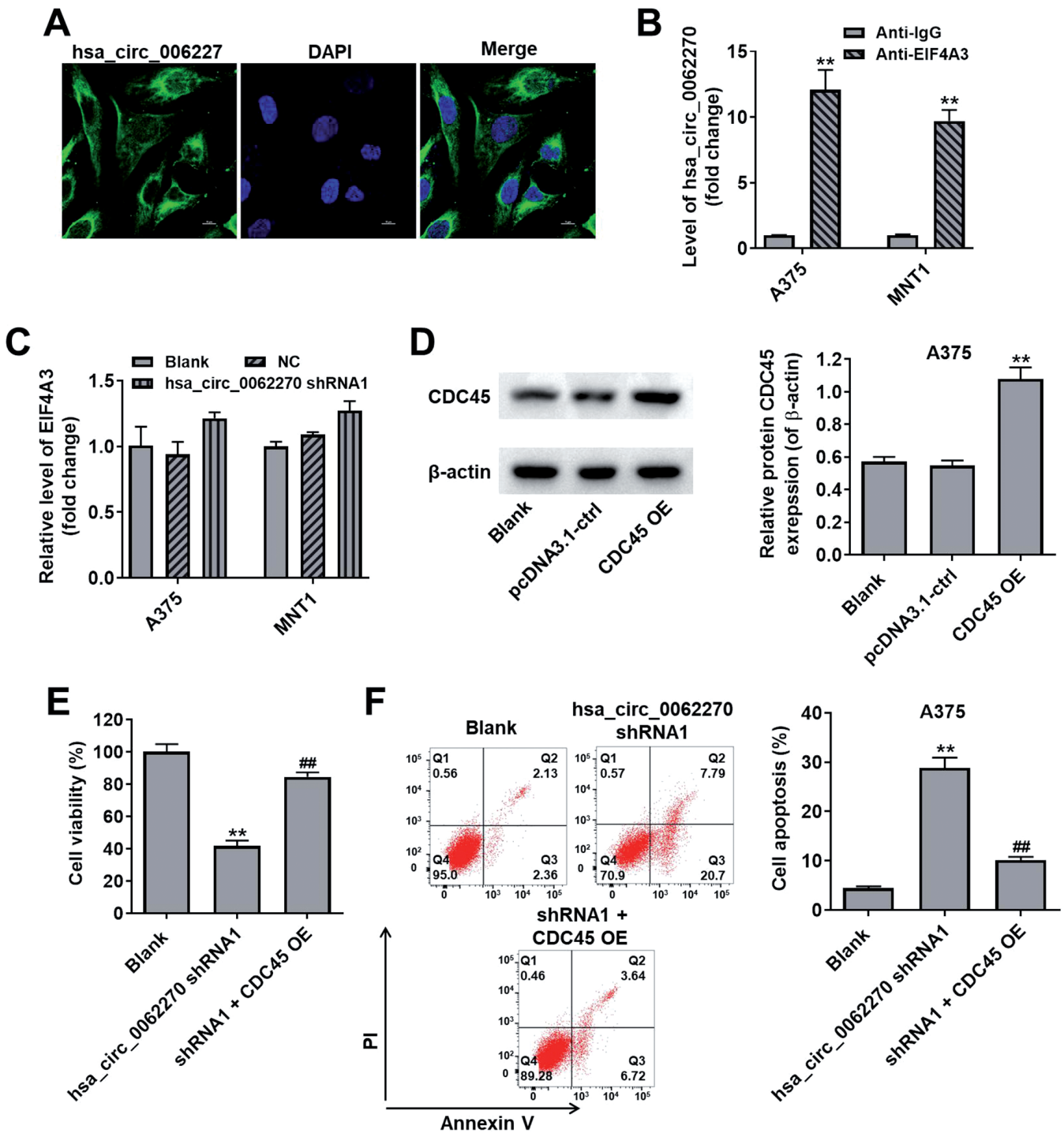

Fig. 5. Hsa_circ_0062270 knockdown inhibited the growth of melanoma cells through downregulation of CDC45. **A.** FISH assay was used to determine the cellular localization of hsa_circ_0062270 in A375 cells. **B.** RIP assay determined the interaction between hsa_circ_0062270 and EIF4A3. RT-qPCR was used to detect enrichment of hsa_circ_0062270. Anti-IgG was used as control. **C.** A375 and MNT1 cells were transfected with NC or hsa_circ_0062270 shRNA1 for 48 h. RT-qPCR assay was used to detect the level of EIF4A3 in A375 cells. **D.** A375 cells were transfected with pcDNA3.1-CDC45 (CDC45 OE) for 48 h. Western blot assay was performed to determine the expression of CDC45 in A375 cells. **E.** A375 cells were transfected with hsa_circ_0062270 shRNA1 or co-transfected with hsa_circ_0062270 shRNA1 and pcDNA3.1-CDC45 for 48 h. CCK-8 assay was used to determine the cell viability. **F.** Apoptosis assay was performed. Cell apoptosis rate was quantified. **P<0.01 compared with blank group. ##P<0.01 compared with hsa_circ_0062270 shRNA1 group. N=3 per group.

6E). Taking these results together, downregulation of hsa_circ_0062270 was able to inhibit the growth of melanoma cells through downregulation of CDC45.

Hsa_circ_0062270 knockdown inhibited tumor growth in a mouse xenograft model

A mouse xenograft model was established to evaluate the role of hsa_circ_0062270 in regulating the melanoma tumor growth in vivo. Since hsa_circ_0062270 shRNA1 achieved better effect of pro-apoptosis and an-invasion in A375 cells (Fig. 3), A375 cells were selected for in vivo study. As shown in Fig. 7A-C, hsa_circ_0062270 shRNA1 significantly inhibited the tumor volume and tumor weight of A375 subcutaneous xenografts, compared with control group. These results of in vivo study demonstrated that hsa_circ_0062270 knockdown was able to inhibit the tumorigenesis of melanoma in vivo.

Discussion

Melanoma is the most aggressive form of skin cancer, the incidence of which has climbed over the past several decades (Chhabra et al., 2017; Matthews et al., 2017; Coricovac et al., 2018). Although early stage melanoma can be surgically removed with good prognosis, the treatment options for advanced melanoma

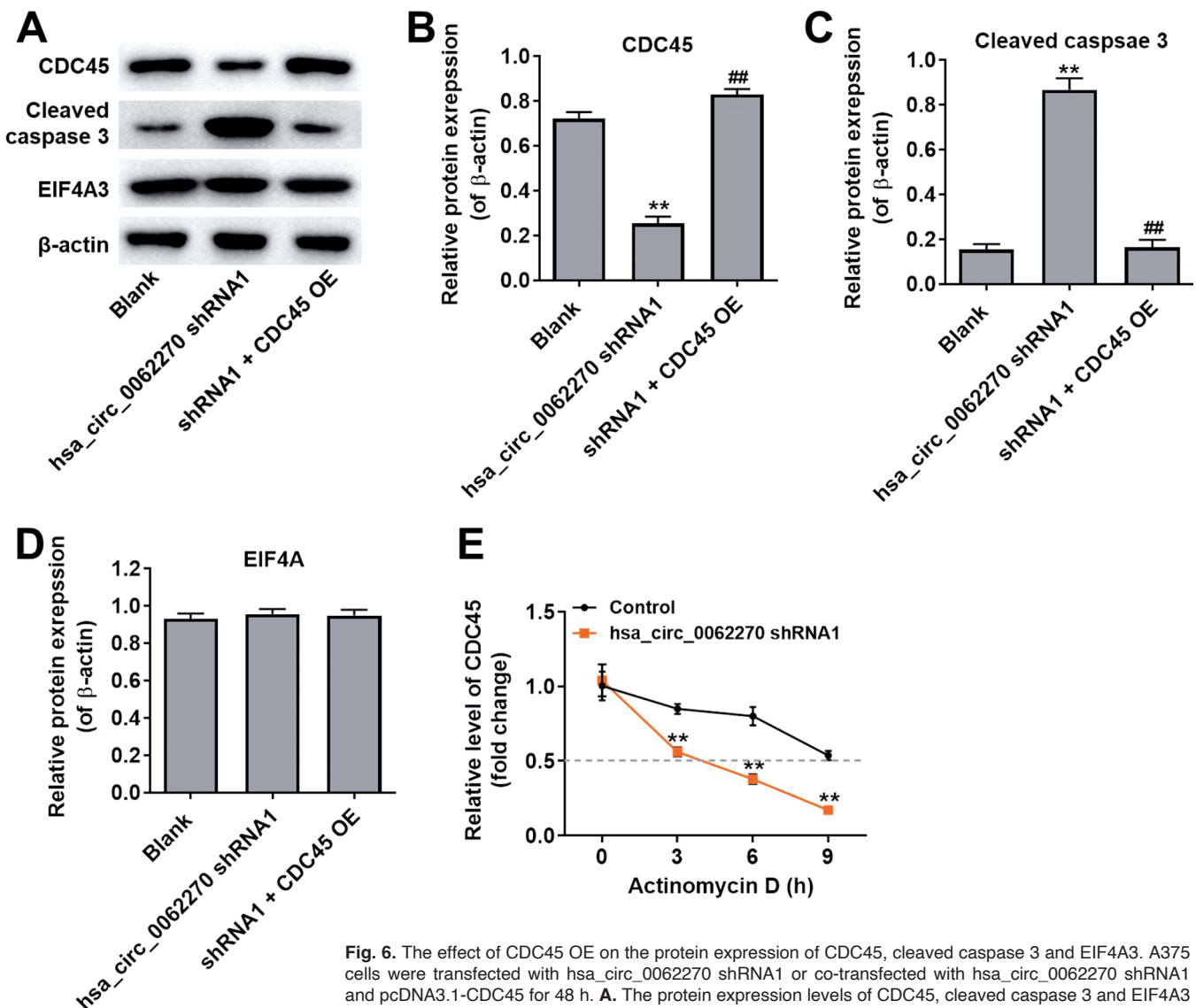

Fig. 6. The effect of CDC45 OE on the protein expression of CDC45, cleaved caspase 3 and EIF4A3. A375 cells were transfected with hsa_circ_0062270 shRNA1 or co-transfected with hsa_circ_0062270 shRNA1 and pcDNA3.1-CDC45 for 48 h. **A.** The protein expression levels of CDC45, cleaved caspase 3 and EIF4A3 were determined using western blot assay. **B-D.** The protein expressions of CDC45, cleaved caspase 3 and EIF4A3 were quantified respectively. **E.** The mRNA stability of CDC45 in actinomycin D-treated melanoma cells was analyzed by RT-qPCR. **P<0.01 compared with blank or control group. ##P<0.01 compared with hsa_circ_0062270 shRNA1 group. N=3 per group.

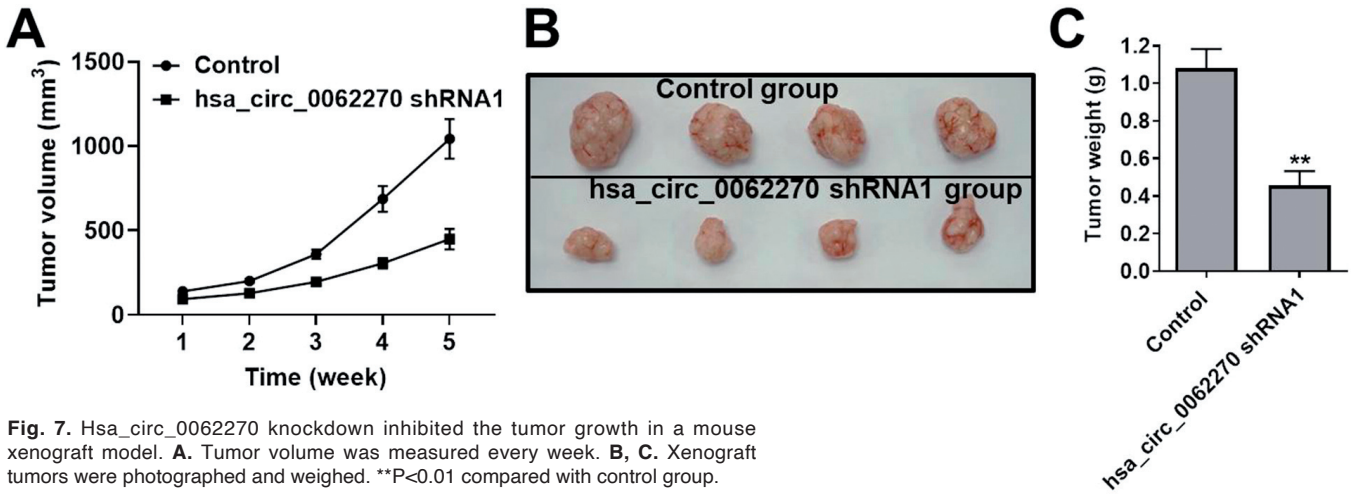

Fig. 7. Hsa_circ_0062270 knockdown inhibited the tumor growth in a mouse xenograft model. **A.** Tumor volume was measured every week. **B, C.** Xenograft tumors were photographed and weighed. **P<0.01 compared with control group.

are still limited (Coricovac et al., 2018). Thus, the identification of new therapeutic targets is essential to improve prognosis of patients with melanoma. To the best of our knowledge, the research on hsa_circ_0062270 is very limited. Bian et al found that hsa_circ_0062270 was upregulated in patients with melanoma (Bian et al., 2018). In line with the previous findings of Bian et al. we confirmed that the level of hsa_circ_0062270 was upregulated in A375 and MNT1 cells compared with normal melanocytes. In addition, our findings, for the first time, uncovered the underlying mechanisms by which hsa_circ_0062270 regulates the progression of melanoma.

In the present study, our findings demonstrated that downregulation of hsa_circ_0062270 decreased the gene and protein expression of CDC45. Meanwhile, hsa_circ_0062270 interacted with EIF4A3 without affecting the relative gene level of EIF4A3. It has been shown that circRNAs can regulate gene expression at transcriptional level via interacting with RBPs (Abdelmohsen et al., 2017). Feng et al indicated that circRNA circ0005276 can promote the progression of prostate cancer via interacting with FUS to activate the transcription of its host gene XIAP (Feng et al., 2019). Thus, we deduce that through interaction with its RBP EIF4A3, hsa_circ_0062270 may stabilize the mRNA of its parental gene CDC45. As expected, our data indicated that hsa_circ_0062270 silencing can decrease the mRNA stability of CDC45. On the other hand, a similar mechanism was also reported in other previous studies. In a study of Zou et al, LINC00324 promoted the proliferation of gastric cancer cells via combing with the RBP human antigen R and thus stabilizing the expression of FAM83B (Zou et al., 2018). Moreover, Bao et al reported that long noncoding RNA CERS6□AS1 promoted breast cancer through binding to its RNA binding protein IGF2BP3 via promoting CERS6 mRNA stability (Bao et al., 2020). Similarly, lncRNA EGFR-AS1 enhanced the malignant phenotype of renal cancer cells (Wang et al., 2019). In this progress, EGFR-AS1 interacted with HuR, which was responsible for the mRNA stability of EGFR (Wang et al., 2019). All these previous findings were in line with our findings. Meanwhile, hsa_circ_0062270 interacted with EIF4A3 without affecting the expression of EIF4A3. However, the detailed mechanism by which the complex of EIF4A3 and hsa_circ_0062270 stabilize the mRNA of CDC45 remains to be further explored.

In the present study, we found that knockdown of hsa_circ_0062270 suppressed the progression of melanoma both in vitro and in vivo via downregulation of CDC45. Therefore, hsa_circ_0062270 might be a therapeutic target for the treatment of melanoma.

Conflicts of interest. The authors declare no competing financial interests.

Author contributions. Zhanpeng Luo conceived and supervised the study; Tian Hao, Yi Yang, Juan He, Jia Bai and Yongjian Zheng designed and performed the experiments. All authors reviewed the results and approved the final version of the manuscript.

References

Abdelmohsen K., Panda A.C., Munk R., Grammatikakis I., Dudekula D.B., De S., Kim J., Noh J.H., Kim K.M., Martindale J.L. and Gorospe M. (2017). Identification of HuR target circular RNAs uncovers suppression of PABPN1 translation by CircPABPN1. RNA Biol. 14, 361-369.

Bao G., Huang J., Pan W., Li X. and Zhou T. (2020). Long noncoding RNA CERS6-AS1 functions as a malignancy promoter in breast cancer by binding to IGF2BP3 to enhance the stability of CERS6 mRNA. Cancer Med. 9, 278-289.

Bian D., Wu Y. and Song G. (2018). Novel circular RNA, hsa_circ_0025039 promotes cell growth, invasion and glucose metabolism in malignant melanoma via the miR-198/CDK4 axis. Biomed. Pharmacother. 108, 165-176.

Cheng X.Y. and Shen H. (2018). Circular RNA in lung cancer research:

Biogenesis, functions and roles. Zhongguo Fei Ai Za Zhi. 21, 50-56 (in chinese).

Chhabra G., Ndiaye M.A., Garcia-Peterson L.M. and Ahmad N. (2017). Melanoma chemoprevention: Current status and future prospects. Photochem. Photobiol. 93, 975-989.

Colaprico A., Silva T.C., Olsen C., Garofano L., Cava C., Garolini D., Sabedot T.S., Malta T.M., Pagnotta S.M., Castiglioni I., Ceccarelli M., Bontempi G. and Noushmehr H. (2016). TCGAbiolinks: an R/Bioconductor package for integrative analysis of TCGA data. Nucleic Acids Res. 44, e71.

Coricovac D., Dehelean C., Moaca E.A., Pinzaru I., Bratu T., Navolan D. and Boruga O. (2018). Cutaneous melanoma - A long road from experimental models to clinical outcome: A review. Int. J. Mol. Sci. 19, 1566.

Feng Y., Yang Y., Zhao X., Fan Y., Zhou L., Rong J. and Yu Y. (2019). Circular RNA circ0005276 promotes the proliferation and migration of prostate cancer cells by interacting with FUS to transcriptionally activate XIAP. Cell Death Dis. 10, 792.

Fiedler J., Baker A.H., Dimmeler S., Heymans S., Mayr M. and Thum T. (2018). Non-coding RNAs in vascular disease - from basic science to clinical applications: scientific update from the Working Group of Myocardial Function of the European Society of Cardiology. Cardiovasc. Res. 114, 1281-1286.

Hsiao K.Y., Sun H.S. and Tsai S.J. (2017). Circular RNA - New member of noncoding RNA with novel functions. Exp. Biol. Med. (Maywood, N.J.). 242, 1136-1141.

Legnini I., Di Timoteo G., Rossi F., Morlando M., Briganti F., Sthandier O., Fatica A., Santini T., Andronache A., Wade M., Laneve P., Rajewsky N. and Bozzoni I. (2017). Circ-ZNF609 is a circular RNA that can be translated and functions in myogenesis. Mol. Cell 66, 22-37.

Liu Q. and Dong H. (2021). EIF4A3-mediated hsa_circ_0088088 promotes the carcinogenesis of breast cancer by sponging miR-135-5p. J. Biochem. Mol. Toxicol. e22909.

Matthews N.H., Li W.Q., Qureshi A.A., Weinstock M.A. and Cho E. (2017). Epidemiology of Melanoma. In: Cutaneous Melanoma: Etiology and Therapy. Ward W.H. and Farma J.M. (eds). Codon Publications. Brisbane (AU).

Maverakis E., Cornelius L.A., Bowen G.M., Phan T., Patel F.B., Fitzmaurice S., He Y., Burrall B., Duong C., Kloxin A.M., Sultani H., Wilken R., Martinez S.R. and Patel F. (2015). Metastatic melanoma - a review of current and future treatment options. Acta Derm. Venereol. 95, 516-524.

Nie H., Wang Y., Liao Z., Zhou J. and Ou C. (2020). The function and mechanism of circular RNAs in gastrointestinal tumours. Cell Prolif. 53, e12815.

Patop I.L., Wüst S. and Kadener S. (2019). Past, present, and future of circRNAs. EMBO J. 38, e100836.

Qu S., Zhong Y., Shang R., Zhang X., Song W., Kjems J. and Li H. (2017). The emerging landscape of circular RNA in life processes. RNA Biol. 14, 992-999.

Rybak-Wolf A., Stottmeister C., Glažar P., Jens M., Pino N., Giusti S., Hanan M., Behm M., Bartok O., Ashwal-Fluss R., Herzog M., Schreyer L., Papavasileiou P., Ivanov A., Öhman M., Refojo D., Kadener S. and Rajewsky N. (2015). Circular RNAs in the mammalian brain are highly abundant, conserved, and dynamically expressed. Mol. Cell 58, 870-885.

Salzman J. (2016). Circular RNA expression: Its potential regulation and function. Trends Genet. TIG. 32, 309-316.

Sanger H.L., Klotz G., Riesner D., Gross H.J. and Kleinschmidt A.K. (1976). Viroids are single-stranded covalently closed circular RNA molecules existing as highly base-paired rod-like structures. Proc. Natl. Acad. Sci. USA 73, 3852-3856.

Starke S., Jost I., Rossbach O., Schneider T., Schreiner S., Hung L.H. and Bindereif A. (2015). Exon circularization requires canonical splice signals. Cell Rep. 10, 103-111.

Tang Z., Li C., Kang B., Gao G., Li C. and Zhang Z. (2017). GEPIA: a web server for cancer and normal gene expression profiling and interactive analyses. Nucleic Acids Res. 45, W98-W102.

Vo J.N., Cieslik M., Zhang Y., Shukla S., Xiao L., Zhang Y., Wu Y.M., Dhanasekaran S.M., Engelke C.G., Cao X., Robinson D.R., Nesvizhskii A.I. and Chinnaiyan A.M. (2019). The landscape of circular RNA in cancer. Cell 176, 869-881.

Wang A., Bao Y., Wu Z., Zhao T., Wang D., Shi J., Liu B., Sun S., Yang F., Wang L. and Qu L. (2019). Long noncoding RNA EGFR-AS1 promotes cell growth and metastasis via affecting HuR mediated mRNA stability of EGFR in renal cancer. Cell Death Dis. 10, 154.

Wang X., Chen M. and Fang L. (2021). hsa_circ_0068631 promotes breast cancer progression through c-Myc by binding to EIF4A3. Mol. Ther. Nucleic Acids 26, 122-134.

Zhang H., Shen Y., Li Z., Ruan Y., Li T., Xiao B. and Sun W. (2020). The biogenesis and biological functions of circular RNAs and their molecular diagnostic values in cancers. J. Clin. Lab. Anal. 34, e23049.

Zhao B., Chen Y., Hu S., Yang N., Wang M., Liu M., Li J., Xiao Y. and Wu X. (2019a). Systematic analysis of non-coding RNAs involved in the angora rabbit (*Oryctolagus cuniculus*) hair follicle cycle by RNA sequencing. Front. Genet. 10, 407.

Zhao X., Cai Y. and Xu J. (2019b). Circular RNAs: Biogenesis, mechanism, and function in human cancers. Int. J. Mol. Sci. 20, 3926.

Zou Z., Ma T., He X., Zhou J., Ma H., Xie M., Liu Y., Lu D., Di S. and Zhang Z. (2018). Long intergenic non-coding RNA 00324 promotes gastric cancer cell proliferation via binding with HuR and stabilizing FAM83B expression. Cell Death Dis. 9, 717.

Accepted December 21, 2021